Journal of the Korean Magnetic Resonance Society **1999**, *3*, 109-126

Adsorbate Interactions of Cu(II) Ion-Exchanged into Mesoporous Aluminosilicate MCM-41 Analyzed by Electron Spin Resonance and Electron Spin Echo Modulation

Jeong Yeon Kim and Jong-Sung Yu*

Department of Chemistry, Hannam University, Taejon, Chungnam, 300-791, Korea
Received September 8, 1999

Abstract: The location of Cu(II) exchanged into mesoporous aluminosilicate MCM-41(AlMCM-41) material and its interaction with various adsorbate molecules were investigated by electron spin resonance and electron spin echo modulation spectroscopies. Cu(II) is fully coordinated to adsorbates in a wide open mesopore of AlMCM-41 for the formation of favorable complexes. It was found that in the fresh hydrated material, Cu(II) is octahedrally coordinated to six water molecules as evidenced by an isotropic room temperature ESR signal. This species is located in a cylindrical MCM-41 channel and rotates rapidly at room temperature. Evacuation at room temperature removes some of these water molecules, leaving the Cu(II) coordinated to less water molecules and anchored to oxygens in an MCM-41 channel wall. Dehydration at 450 °C produces one Cu(II) species located on the internal wall of a channel, which is easily accessible to adsorbates. Adsorption of adsorbate molecules such as water, methanol, ammonia, pyridine, aniline, acetonitrile, benzene, and ethylene on a dehydrated Cu-AlMCM-41 material causes changes in the ESR spectrum of Cu(II), indicating the complex formation with these adsorbates. Cu(II) forms a complex with six molecules of methanol as evidenced by an isotropic room temperature ESR signal and ESEM analysis like upon water adsorption. Cu(II) also forms a square planar complex containing four molecules of N-containing adsorbates such as ammonia, pyridine and aniline based on resolved nitrogen superhyperfine interaction and their ESR parameters. However, Cu(II) forms a complex with six-molecules of acetonitrile based on ESR parameters. Only one molecule of benzene or ethylene is coordinated to Cu(II).

INTRODUCTION

Recently, a new class of mesoporous materials with a hexagonal array of parallel one dimensional channels, designated as MCM-41 has been reported by Mobil scientists[1,2] The novelty in synthesis of the MCM-41 is the use of surfactant micelles around which silicates

polymerize hydrothermally to form the matrix structure. An exciting property of these materials is the possibility to control the pore size in the range between 2 nm and 10 nm by using surfactants with different molecular sizes and auxiliary organic species during crystallization process.[3,4] The large channel diameter and its tailorability provide new opportunities for adsorptive and catalytic applications including large molecules.[3-5]

It has been reported that MCM-41 aluminosilicates can be synthesized with different Si/Al ratios of 2.5 and higher.[6,7] But the synthetic methods incorporating Al to a pure silica framework often hindered by a severe decrease in the structural order as Al content increases.[7] Besides, the line widths of XRD patterns and ^{29}Si NMR spectra may increase upon calcination, indicating a collapse of a long range structural order.[1-7] Variability in the long-range structural order greatly inhibits not only the interpretation of spectroscopic or other characterization studies of these materials, but also restricts practical applications requiring structural integrity. Several synthetic approaches were proposed to improve the thermal and hydrothermal stability and long-range structural order of AlMCM-41 materials.[4,8,9] Al-containing MCM-41 materials have been found to exhibit ion-exchange capacity and acidity comparable to those of aluminosilicate zeolites.[10-12]

In this work, mesoporous AlMCM-41 materials with superior structural order are synthesized, and paramagnetic probe Cu(II) ions have been ion-exchanged into the MCM-41 aluminosilicate framework by a liquid state procedure to investigate the location of probe Cu(II) in the AlMCM-41 and its interaction with adsorbates by electron spin resonance(ESR) and electron spin echo modulation(ESEM) spectroscopies.

EXPERIMENTAL SECTION

Synthesis and Ion Exchange

Mesoporous AlMCM-41 materials with high structural integrity and improved textural uniformity have been synthesized according to the modification of synthetic methods of Ryoo et al.[8] A surfactant source was obtained by dissolving dodecyltrimethylammonium(DTA) bromide (from Aldrich) and tetrapropylammonium (TPA) bromide (from Aldrich) in a mixture of aqueous solution of hexadecyltrimethylammonium chloride (HTACl), aqueous NH_3 solution, and doubly distilled water. A clear solution of sodium silicate was prepared by combining aqueous NaOH solution with colloidal silica, Ludox HS40(39.5 wt% SiO_2, 0.4 wt% Na_2O and 60.1 wt% H_2O, from Aldrich) and heating the resulting gel mixture with stirring for 2 h at 353 K. Alumina source was a solution of sodium aluminate desolved in doubly distilled water.

The silicate solution was dropwise added to the surfactant source with vigorous stirring at room temperature. After the resulting surfactant-silicate gel mixture was stirred for 1 h at room temperature, the sodium aluminate solution was dropwise added with vigorous stirring. The resulting surfactant-aluminosilicate gel mixture had bulk molar composition of 6.00 SiO_2:0.08 Al_2O_3:1.00 HTACl:0.25 DTABr:0.25 TPABr: 0.16$(NH_4)_2O$:

1.50 Na_2O: 302 H_2O with theoretical Si/Al ratio of 40. The gel mixture was stirred for 30 min more to form an homogeneous mixture before heating in oven at 373 K for 1 day. The HTA-aluminosilicate mixture was then cooled to room temperature. Subsequently, pH of the reaction mixture was adjusted to 10.2 by dropwise addition of 30 wt% acetic acid with vigorous stirring. The reaction mixture after the pH adjustment was heated again to 373 K for 1 day. This procedure for pH adjustment to 10.2 and subsequent heating for 1 day was repeated twice more. The precipitated product, AlMCM-41with HTA template, was filtered, washed with doubly distilled water, and dried at room temperature. The dried AlMCM-41 product was stirred in an ethanol-hydrochloric acid mixture(0.1 mol of HCl/ L of ethanol) for 1 h under reflux conditions. Subsequently, the product was washed with ethanol and dried at room temperature. Calcination of the product was carried out in O_2 flow while the sample was heated to 813 K over 10 h and maintained at this temperature for 10 h. Elemental analysis for the Si/Al ratios was performed with inductively coupled plasma(ICP) emission spectroscopy. AlMCM-41 sample gave Si/Al ratios of 43.6, which is close to the expected bulk Si/Al ratio.

The surfactant-free mesoporous AlMCM-41 was then exchanged at room temperature for 12 h by dropwise addition of a 10 mM solution of cupric nitrate (Alfa Products) according to the procedure described earlier.[13] Copper exchange was 1.8 - 2.6 % by weight of calcined AlMCM-41, assuming complete exchange. Sample prepared in this manner is termed as a fresh, hydrated Cu-AlMCM-41.

Sample Treatment

The aluminosilicate sample was loaded directly into a Suprasil quartz ESR tube (2 mm i.d. by 3 mm o.d.) reactor which could be connected to a vacuum and gas handling line. Dehydration of the sample was carried out by first evacuating the sample at room temperature followed by heating to 400°C over an 8～10 h period in a static reactor. Following this evacuation the sample was exposed to 200～400 Torr of static high-purity dry oxygen for 5～10 h at 450°C in order to oxidize any copper species that had been reduced during the heating period. Finally, the oxygen was pumped off at room temperature under a 10^{-5} Torr vacuum. This heat treated sample with oxygen is termed as a dehydrated sample.

After dehydration, adsorbates as gases were admitted at room temperature to the sample tubes and left to equilibrate. Deuterated adsorbates such as D_2O and CH_3OD, C_2D_4, C_6D_6 and other isotope substituted adsorbate, $^{15}NH_3$, were obtained from Aldrich and used after repeated freeze-pump-thaw cycles.

Spectroscopic Measurements

Mesoporous AlMCM-41 samples after synthesis, calcination and Cu(II) exchange are examined by powder x-ray diffraction(XRD) with a Philips PW 1840 diffractometer. ESR

spectra were measured both at room temperature and at 77 K on an ESP 300 Bruker spectrometer. ESEM spectra were recorded with a Bruker ESP 380 pulsed ESR spectrometer at 4.5 K. Three-pulse echoes were measured by using a 90°-t-90°-T-90° pulse sequence with the echo measured as a function of T. The parameters to be determined are the number of interacting nuclei(N), the distance(R) between the paramagnetic center Cu(II) and the interacting nuclei, and their isotropic hyperfine interaction(A_{iso}).[14]

RESULTS

X-Ray Diffraction

Powder XRD measurements were performed before and after calcination of as-synthesized AlMCM-41 to confirm that the synthesis product has a MCM-41 structure. The XRD patterns show high structural order with at least four clearly resolved signals corresponding to d_{100}, d_{110}, d_{200} and d_{210} as shown in Fig. 1, indicating the existence of the hexagonal MCM-41 phase. The spectrum shows an intense peak at $2\theta = 2.1°$ which corresponds to a spacing about d_{100}= 4.2 nm. Upon calcination, the intense peak slightly shi-

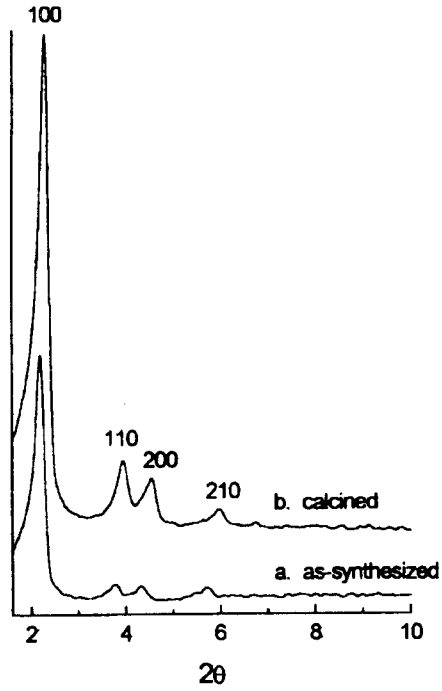

Fig. 1. X-ray powder diffraction patterns of (a) an as-synthesized and (b) a calcined AlMCM-41.

fts to a higher angle $2\theta = 2.3°$, corresponding to a spacing of $d_{100} = 3.9$ nm. The intensity of the signals upon calcination increases to more than twice that in as-synthesized AlMCM-41. There are no significant changes of XRD patterns after Cu(II) exchange and dehydration.

Electron Spin Resonance

The Cu(II) ESR spectral measurements at 77 K and at room temperature of fresh, hydrated Cu-AlMCM-41 are illustrated in Fig. 2. The fresh, hydrated sample measured at 77 K before evacuation produces an anisotropic ESR signal, denoted as species A characteristic of an axial powder spectrum of Cu(II) as shown in Fig. 2b. Species A has ESR parameters of $g_{\|} = 2.411$ and $A_{\|} = 141 \times 10^{-4}$ cm^{-1}. The hyperfine lines of the perpendicular component are not resolved. A value of $g_{\perp} = 2.08$ was estimated for the perpendicular component of the g tensor. The ESR spectrum measured at room temperature of the fresh, hydrated Cu-AlMCM-41, however, shows an almost isotropic signal at $g_{iso} = 2.188$ with Δ Hpp = 146 G as shown in Fig. 2a. Evacuation at room temperature decreases the isotropic ESR signal of the fresh, hydrated Cu-AlMCM-41 sample. After about 1.5～3 h evacuation at room temperature, the isotropic signal is no longer observed in the room temperature ESR spectrum. The ESR spectrum measured at 77 K after evacuation at room temperature for 2 h shows a development of another new species, denoted as B which has $g_{\|} = 2.387$, $A_{\|} = 152 \times 10^{-4}$ cm^{-1} and $g_{\perp} = 2.08$ as shown in Fig. 2c.

Fig. 3a illustrate the development of a new Cu(II) species D after dehydration with ESR parameters of $g_{\|} = 2.316$, $A_{\|} = 177 \times 10^{-4}$ cm^{-1} and $g_{\perp} = 2.07$. Upon adsorption of 150 Torr of oxygen at room temperature into dehydrated Cu-AlMCM-41 sample, the ESR signals of the Cu(II) species were found to be broadened. Evacuation of excess oxygen recovers the ESR signal intensity of species D. After the dehydration treatment, complete rehydration of the dehydrated sample by exposure to the saturation vapor pressure of water at room temperature regenerates the original species A seen in fresh, hydrated Cu-AlMCM-41 which shows an isotropic room temperature ESR signal (Fig. 2a).

Fig. 3b and 3c show the ESR spectra at 77 K and at room temperature observed after adsorption of methanol on dehydrated Cu-AlMCM-41. Adsorption of methanol produces an anisotropic ESR spectrum at 77 K with $g_{\|} = 2.409$, $A_{\|} = 138 \times 10^{-4}$ cm^{-1} and $g_{\perp} = 2.08$ as shown in Fig. 3b. However, almost an isotropic signal at $g_{iso} = 2.182$ with Δ Hpp =148 G was observed in the ESR spectrum measured at room temperature almost like upon water adsorption (Fig. 3c).

Fig. 4 shows the ESR spectra at 77 K after adsorption of 30 Torr ammonia gas. The color of the sample turns from pale blue to blue after adsorption. Two new cupric ion species due to complex formation with ammonia are observed: a major species with ESR parameters of $g_{\|} = 2.281$ and $A_{\|} = 170 \times 10^{-4}$ cm^{-1}, and another minor species with $g_{\|} = 2.254$ and $A_{\|} = 196 \times 10^{-4}$ cm^{-1}. But the minor species decreases slowly. Cu-AlMCM-41 with adso-

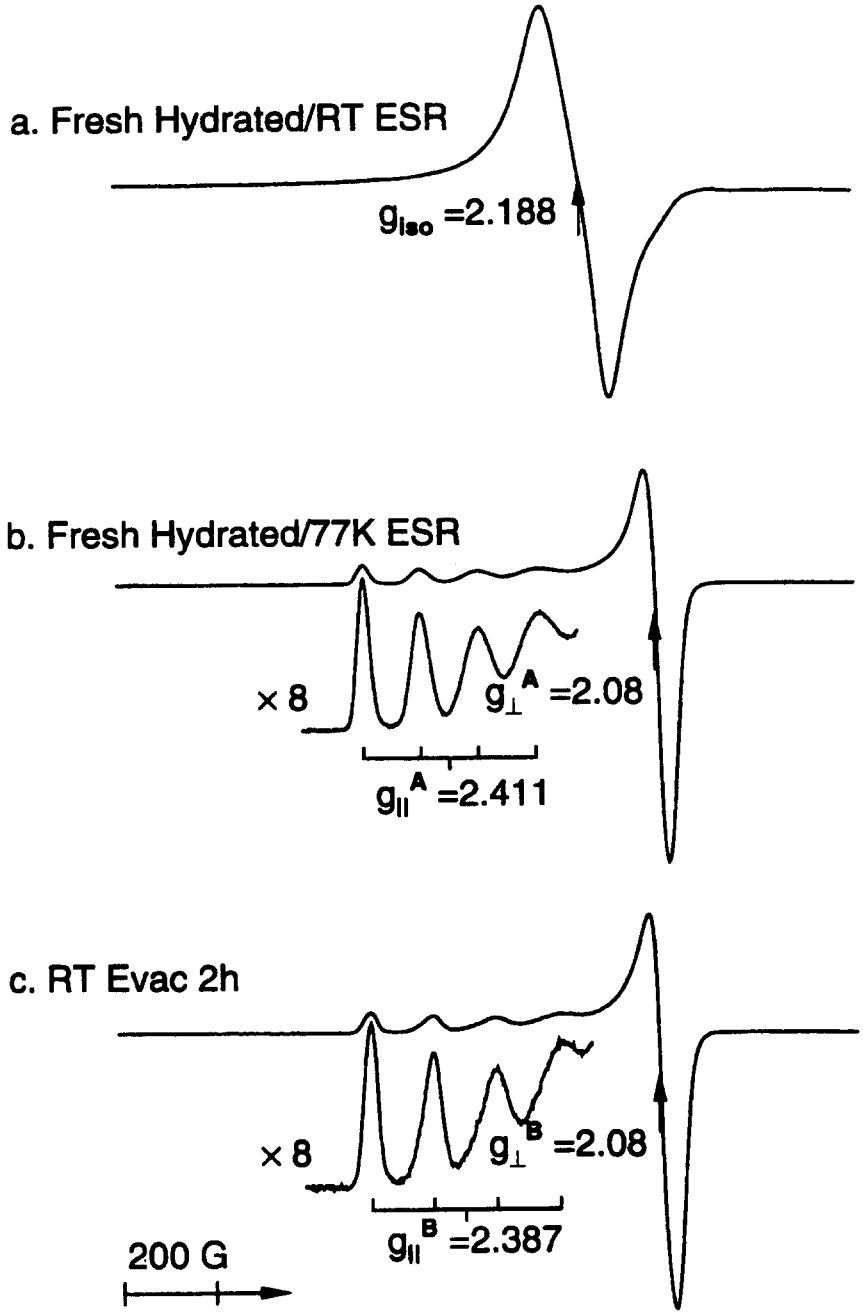

Fig. 2. ESR spectra of fresh hydrated Cu-AlMCM-41 recorded (a) at room temperature, (b) at 77 K and (C) at 77 K after room temperature evacuation for 2 h.

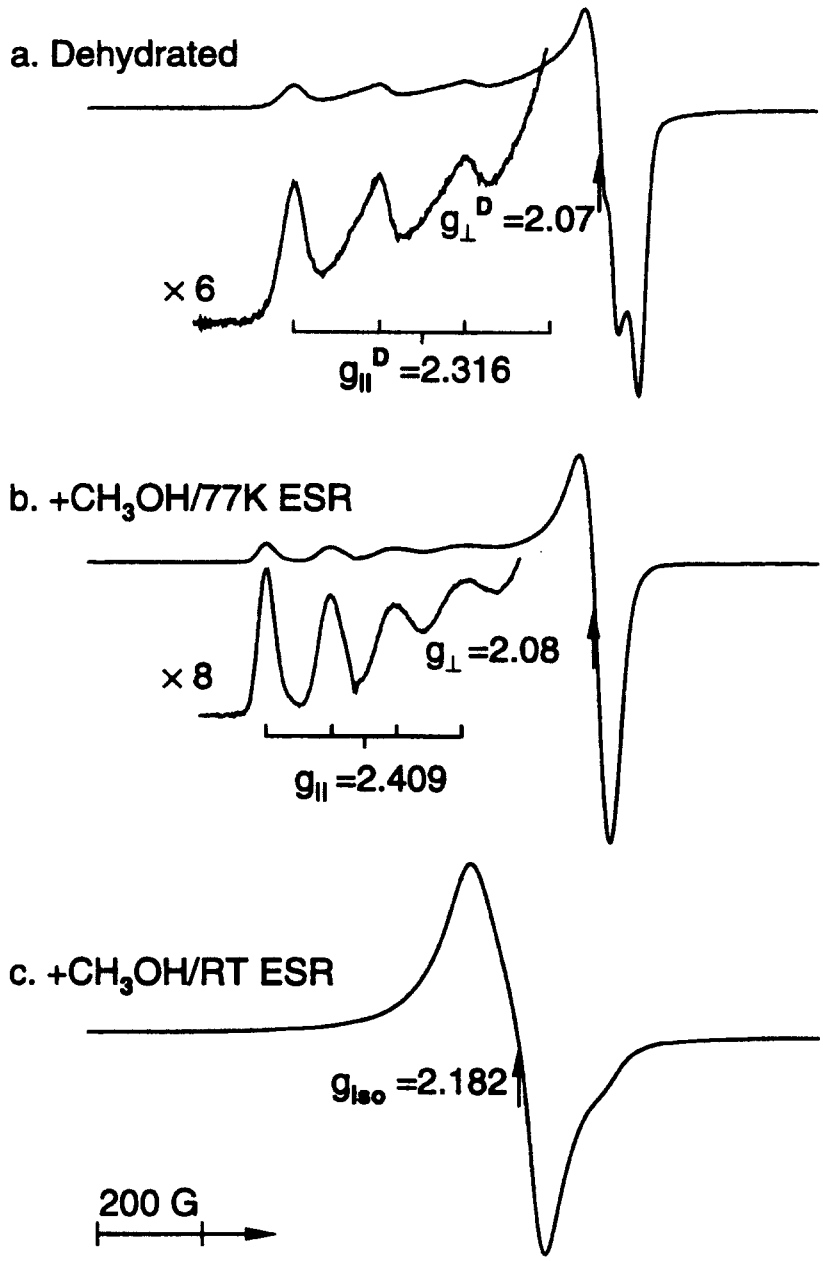

Fig. 3. ESR spectra of Cu-AlMCM-41 measured (a) at 77 K after dehydration, (b) at 77 K and (c) at room temperature after equilibration with methanol following dehydration as in (a).

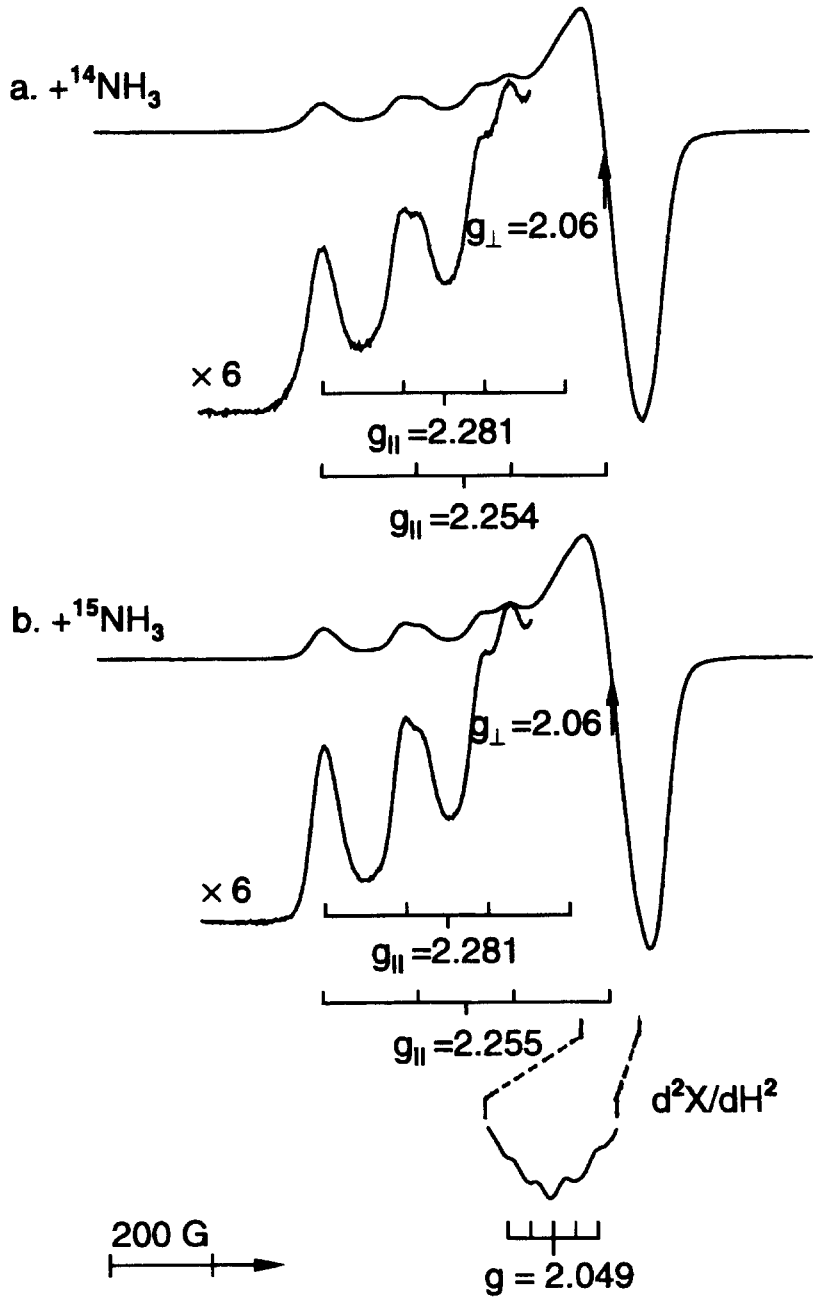

Fig. 4. ESR spectra at 77 K of dehydrated Cu-AlMCM-41 (a) after adsorption of 30 Torr $^{14}NH_3$ and (b) after adsorption of 30 Torr $^{15}NH_3$ at room temperature.

rbed $^{15}NH_3$ (^{15}N has a nuclear spin of 1/2) shows five ^{15}N hyperfine lines centered at g = 2.049 and split by 18 x 10^{-4} cm^{-1} which are shown in the expanded second derivative spectrum. The intensity ratio of the five ^{15}N hyperfine signals is close to the expected ratio of 1:4:6:4:1. With adsorbed $^{14}NH_3$(^{14}N has a nuclear spin of 1), the ESR spectrum shows more hyperfine lines in the $g_\perp$ region, but they are not clearly resolved. Fig. 5 shows ESR profiles after adsorption of N-containing molecules, pyridine, aniline and acetonitrile upon a dehydrated Cu-AlMCM-41 sample. Adsorption of pyridine produces a new cupric ion species with ESR parameters of $g_\parallel$ = 2.285 and $A_\parallel$ = 174 x 10^{-4} cm^{-1}. Upon adsorption of aniline, a new species is observed with ESR parameters of $g_\parallel$ = 2.274 and $A_\parallel$ = 175 x 10^{-4} cm^{-1} similar to those for adsorption of ammonia and pyridine. Upon adsorption of acetonitrile, a new species is also observed but with rather different ESR parameters of $g_\parallel$ = 2.377 and $A_\parallel$ = 154 x 10^{-4} cm^{-1}. But nitrogen hyperfine lines are not resolved in the $g_\parallel$ region from these N-containing ligand molecules.

Fig. 6b shows the ESR spectrum after equilibration of benzene upon a dehydrated sample. A new species occurs with ESR parameters of $g_\parallel$ = 2.376 and $A_\parallel$ = 147 x 10^{-4} cm^{-1}. Upon adsorption of ethylene, a new cupric ion species with ESR parameters of $g_\parallel$ = 2.348 and $A_\parallel$ = 149 x 10^{-4} cm^{-1} is weakly obtained in overlap with major species D (Fig. 6c). The new species is thus considered to be a cupric ion species occurring due to interaction with ethylene. Table 1 summarizes the ESR parameters of Cu(II) in AlMCM-41 studied in present work.

Electron Spin Echo Modulation

Three-pulse ESEM spectra and simulation parameters for Cu(II) in dehydrated Cu-AlMCM-41 interacting with various deuterated adsorbates are shown in Fig. 7 and 8. All ESEM spectra were recorded at the perpendicular spectral region of the Cu(II) powder spectrum. Fig. 8a shows an ESEM spectrum of dehydrated Cu-AlMCM-41 fully hydrated with D_2O which shows an isotropic ESR signal at room temperature. The simulation shown indicates that Cu(II) is interacting with twelve neighboring deuterium nuclei, i.e. six water molecules, with a Cu(II)-D distance of 0.29 nm, which indicates direct coordination.

Fig. 7b shows three-pulse ESEM spectrum of dehydrated Cu-AlMCM-41 with adsorbed CH_3OD. The simulation for CH_3OD indicates interaction with six deuterium nuclei, i.e. six molecules of methanol with a Cu(II)-D distance of 0.29 nm. Fig. 8 shows the three-pulse ESEM spectra and simulation parameters for dehydrated Cu-AlMCM-41 with adsorbed C_6D_6 and C_2D_4. Best simulation shows six interacting deuterium nuclei at a Cu(II)-D distance of 0.43 nm for deuterated benzene adsorption. Shallow deuterium modulation is shown upon adsorption of C_2D_4 (Fig. 8b). The simulation for C_2D_4 adsorption indicates interaction with four deuterium nuclei at a Cu(II)-D distance of 0.52 nm. These results indicate one molecule of benzene or ethylene interacting with Cu(II).

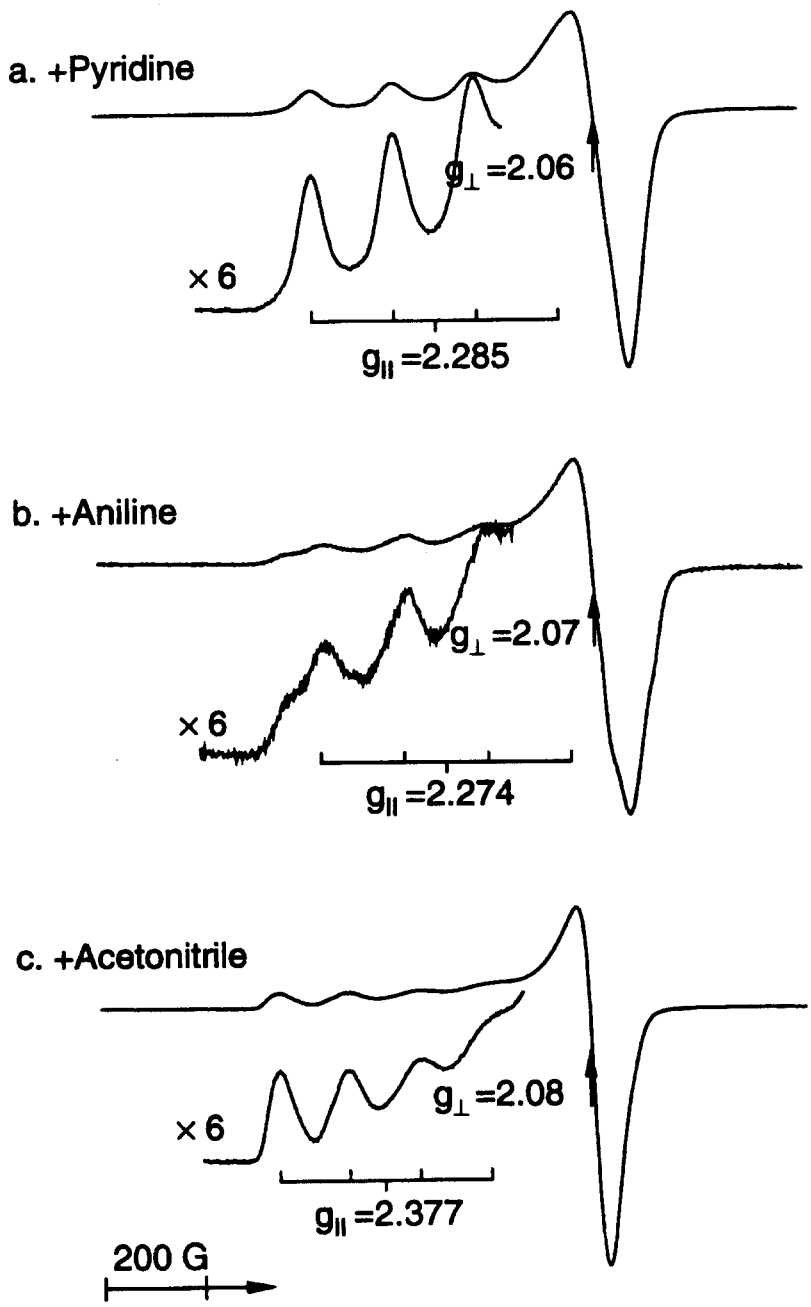

Fig. 5. ESR spectra at 77 K of dehydrated Cu-AlMCM-41 upon adsorption of (a) pyridine, (b) aniline and (c) acetonitrile.

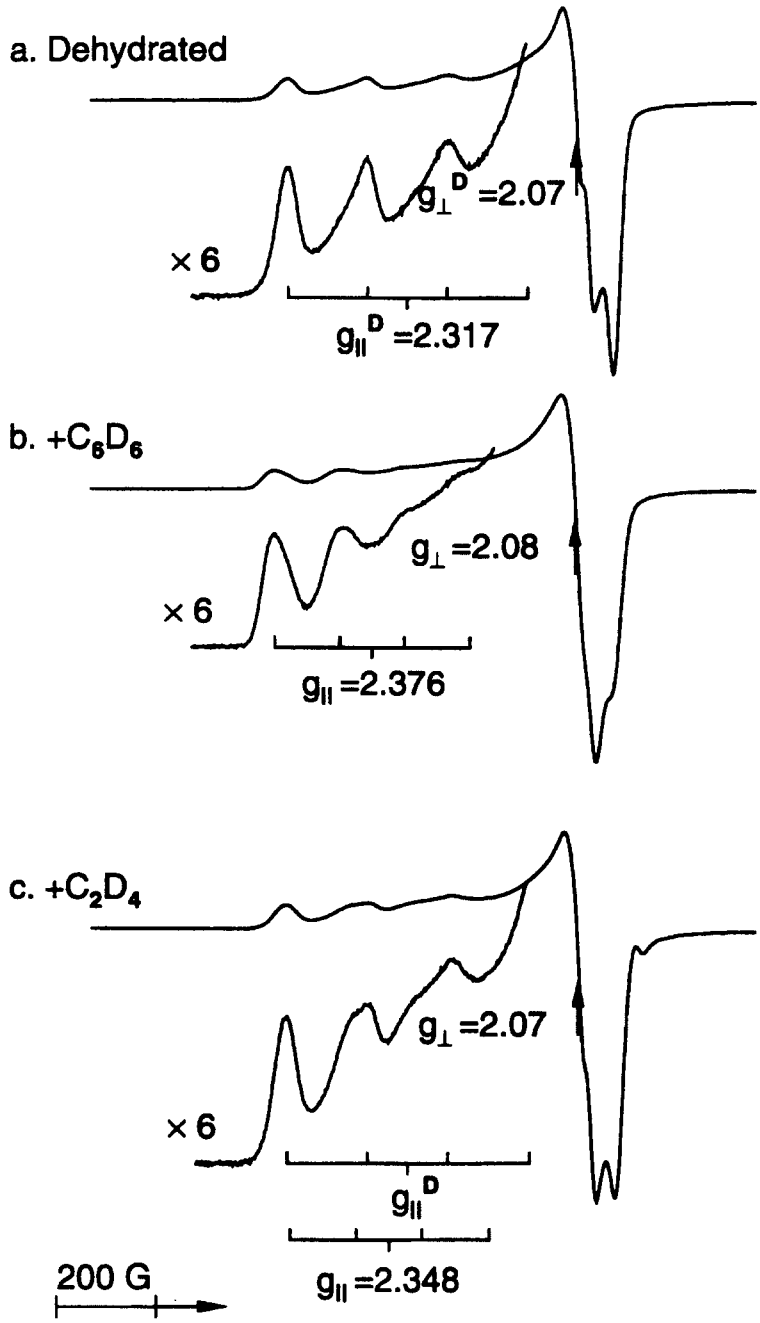

Fig. 6. ESR spectra at 77 K of Cu-AlMCM-41 (a) after dehydration, and after equilibration with (b) benzene and (c) ethylene following the dehydration as in (a).

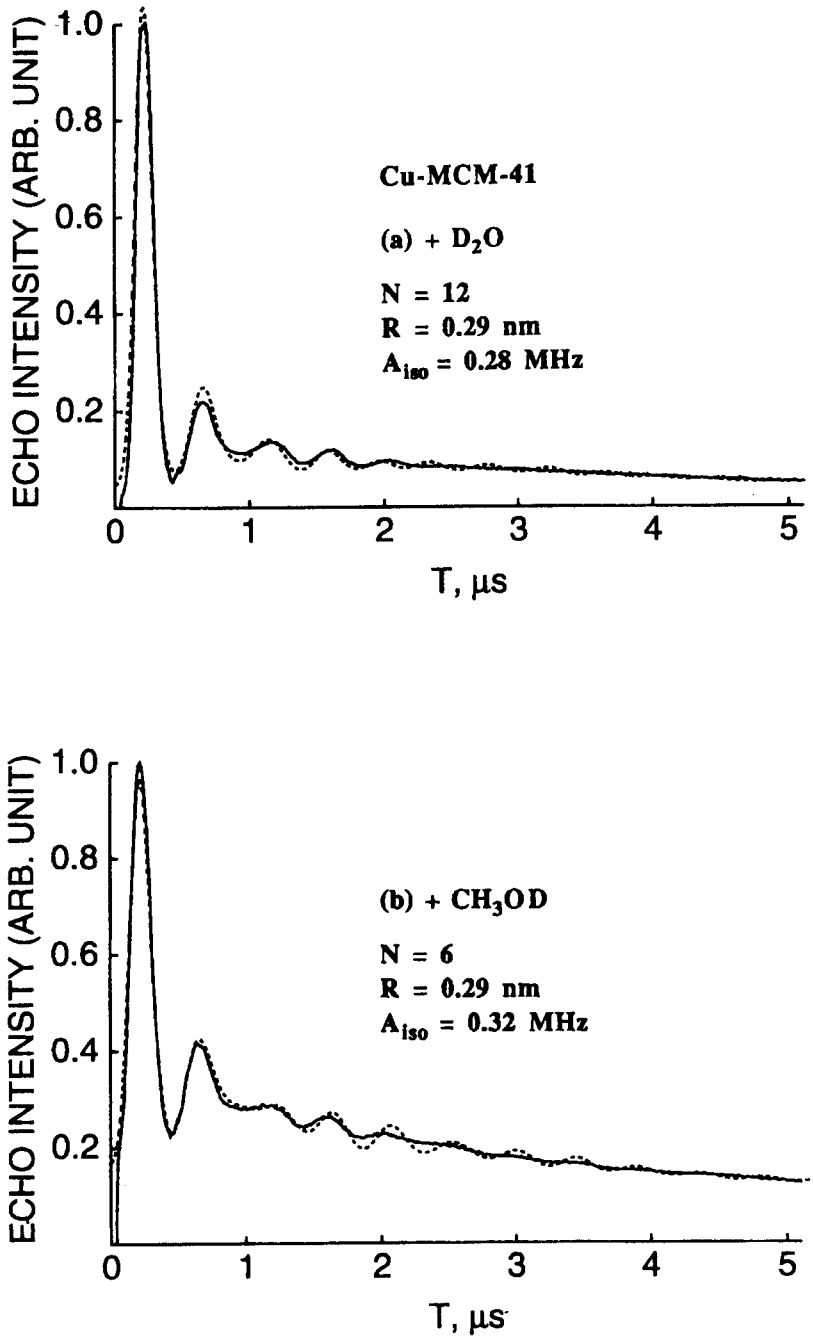

Fig. 7. Experimental (——) and simulated(----) three-pulse ESEM spectra recorded at 4.5 K of dehydrated Cu-AlMCM-41(a) with adsorbed D_2O and (b) with adsorbed CH_3OD.

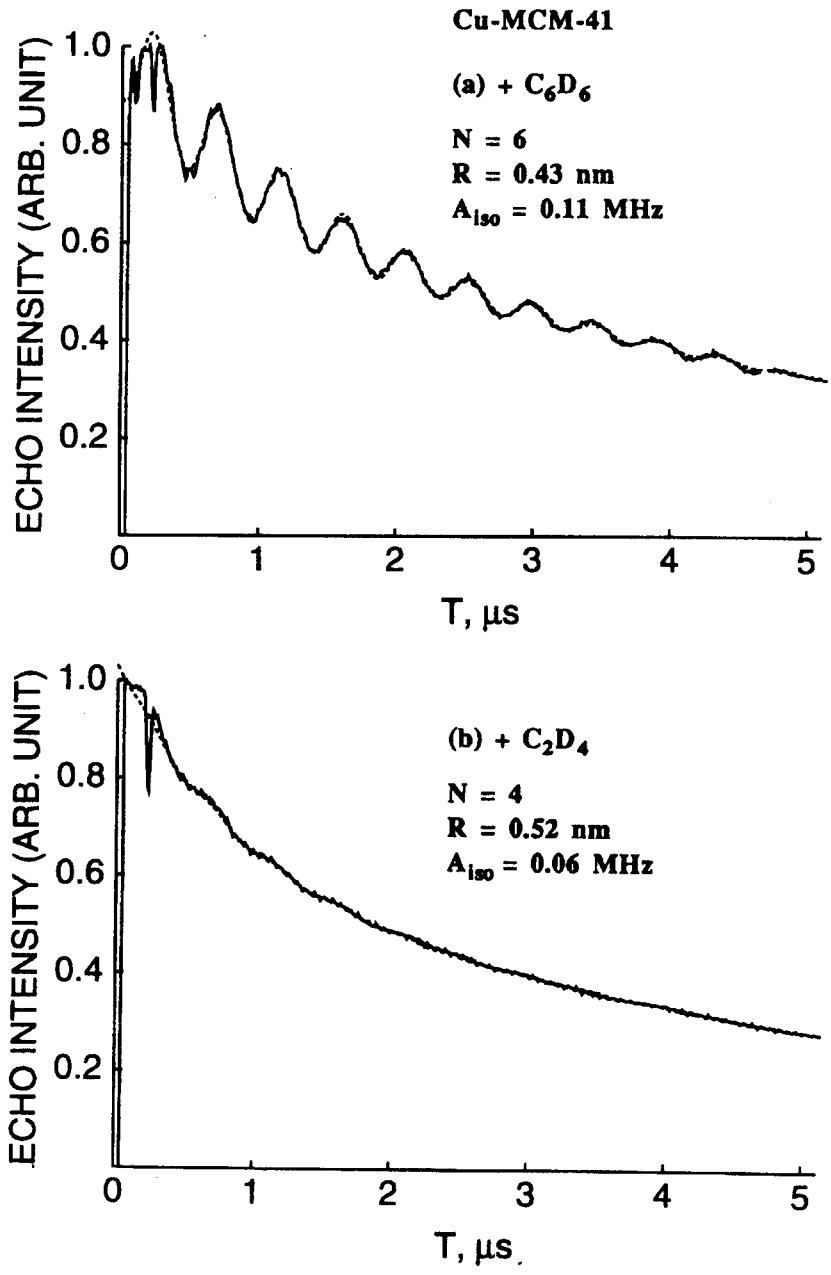

Fig. 8. Experimental (——) and simulated(----) three-pulse ESEM spectra recorded at 4.5 K of dehydrated Cu-AlMCM-41 (a) with adsorbed C_6D_6 and (b) with adsorbed C_2D_4.

Table 1. ESR parameters at 77 K of Cu(II) in Cu-AlMCM-41 after various sample treatments.

treatment[a]	species[b]	$g_{\|}$[c]	$A_{\|}$[d]	$g_{\perp}$[e]
fresh/RT ESR		2.188[f]		
Fresh	A	2.411	141	2.08
evac[a] RT/1.5 h	B	2.387	152	2.08
Dehydrated	D	2.316	177	2.07
$+H_2O$	A	2.411	141	2.08
$+CH_3OH$/RT ESR		2.182[f]		
$+CH_3OH$		2.409	138	2.08
$+NH_3$		2.281	170	2.06
		2.254	196	2.06
+pyridine		2.285	174	2.06
+aniline		2.274	175	2.07
+acetonitrile		2.377	154	2.08
+benzene		2.376	147	2.08
+ethylene		2.348	149	2.07

[a]Evac = evacuated at; RT = room temperature. [b]Multiple species are listed in order of decreasing concentration. [c]Estimated uncertainty is ± 0.007. [d]The unit of $A_{\|}$ is 1 x 10^{-4} cm^{-1} and the estimated uncertainty is ± 6 x 10^{-4} cm^{-1}. [e]Estimated uncertainty is ± 0.01. [f]g_{iso} value.

DISCUSSION

The changes in the ESR parameters of dehydrated Cu-AlMCM-41 after adsorption of various adsorbate molecules indicate that the adsorbates interact with the Cu(II) ion. The Cu(II) spin Hamiltonian parameters usually provide some guide to the overall coordination symmetry of the metal ion site based on extensive studies of known Cu(II) crystalline compounds. In general, $A_{\|}$ increases from ~ 0.007 cm^{-1} for tetrahedral symmetry, through distorted octahedral and square pyramidal symmetry, to ~0.017 cm^{-1} for square-planar symmetry, whereas $g_{\|}$ decreases from 2.516 to 2.245 for this sequence of coordination symmetries.[15,16] Together with the number of adsorbed molecules determined by ESEM and a comparison with known Cu(II) locations in zeolites, the Cu(II) ESR parameters provide information about the coordination and location of Cu(II) ions exchanged into AlMCM-41.

The fresh hydrated Cu-AlMCM-41 gives an ESR spectrum predominantly consisting of a broad isotropic line at ambient temperature (Fig. 2a). Such an isotropic ESR signal at room temperature is indicative of a mobile species which is rotationally unrestricted on the ESR time scale. Analysis of the three-pulse ESEM spectrum (Fig. 7a) of dehydrated alumi-

nosilicate rehydrated with D_2O indicates a water solvation number of six around Cu(II), i.e. $[Cu(H_2O)_6]^{2+}$. A similar broad isotropic ESR signal has been observed at room temperature for Cu(II) in L zeolite[17] and in other zeolites[18,19] and was assigned to $[Cu(H_2O)_6]^{2+}$ from ESR and ESEM analyses. At 77 K this $[Cu(H_2O)_6]^{2+}$ complex becomes immobilized and gives rise to an asymmetric spectrum as shown in Fig. 2b. Mesoporous MCM-41 molecular sieve consists of hexagonal array of cylindrical mesopore channels whose diameter is about 3.0 nm. The internal area of the channel is large enough to accommodate a hexaaquo complex of Cu(II) with a diameter of about 0.67 nm. Thus species A is assigned to a hexaaquo complex of Cu(II), $[Cu(H_2O)_6]^{2+}$, located in a main channel.

When the hydrated sample is evacuated at room temperature, the isotropic ESR component decreases. After 1.5 ~ 3 h of evacuation, the ESR signal shows another species B. This is indicative of the copper losing some water ligands and becoming immobilized by coordination to several lattice oxygens. A resultant loss of mobility in this way leads to the observed g factor anisotropy in the Cu(II) ESR spectrum.

Based on the spin Hamiltonian parameters, the Cu(II) species D after dehydration is likely to have distorted octahedral or square pyramidal symmetry. Species D has a smaller $g_{\|}$ value and a bigger $A_{\|}$ value compared to ESR parameters of the octahedral Cu(II) species A. Since these parameters of species D are rather closer to those of square planar symmetry ($g_{\|}$ = 2.281 and $A_{\|}$ = 170 x 10^{-4} cm^{-1} for a square planar ammonia complex of Cu(II) to be explained below), the Cu(II) species D in dehydrated sample is more likely to have square pyramidal symmetry with one OH from a residual water molecules and four oxygen atoms on the lattice surface of a mesopore or perhaps with five oxygen atoms on the surface of a mesopore than to have distorted octahedral symmetry. After such dehydration, the Cu(II) species show broadening of its ESR lines upon oxygen adsorption at room temperature. Thus Cu(II) species in dehydrated AlMCM-41 is likely to be located on the internal surface of the mosopore which is easily accessible to oxygen. After dehydration, the samples were examined by powder X-ray diffraction and there was no significant change of XRD pattern.

Adsorption of methanol on dehydrated Cu-AlMCM-41 produces an anisotropic ESR spectrum at 77 K of Cu(II) (Fig. 3b). The ESR parameters are comparable to those of species A in a fresh hydrated sample which correspond to octahedral symmetry. However, almost an isotropic signal was observed in room temperature ESR spectrum like upon water adsorption. This also indicates a mobile Cu(II) species, i.e. Cu(II) species octahedrally coordinated with methanol. ESEM analysis also indicates a complex involving six molecules of methanol (Fig. 7b) and supports the assignment of the species to a $[Cu(CH_3OH)_6]^{2+}$.

Adsorption of NH_3 on dehydrated Cu-AlMCM-41 results in two new overlapping Cu(II) species due to complex formation with NH_3 as shown by the changes in its ESR parameters. The major species has ESR parameters($g_{\|}$ = 2.281 and $A_{\|}$ = 170 x 10^{-4} cm^{-1}) comparable to those for pyridine and aniline adsorption. The minor species decreases slowly. The observed five ^{15}N superhyperfine lines with adsorbed $^{15}NH_3$ also indicate four ammonia

molecules coordinated to the Cu(II)(Fig. 4b). Tetracoordinated cupric complexes such as CuX_4(X = Cl, NH_3, etc) generally prefer a square-planar configuration.[21] The $g_{||}$ = 2.281 is slightly higher, but ESR parameters of this species are in general consistent with those of other tetraammmonia complexes of Cu(II).[20,22-28] Thus, in this case the Cu(II) species is suggested to be located in a mesopore channel, coordinating to four ammonia molecules in a square planar geometry. The ESR parameters of tetraammonia complexes formed between Cu(II) and ammonia in various zeolites and molecular sieves are tabulated in Table 2 for comparison.

Other N-containing adsorbate molecules such as pyridine and aniline produces ESR parameters similar to those for NH_3 adsorption. In this case, Cu(II) is also suggested to be located in a mesopore channel, coordinating to four molecules of pyridine or aniline in a square planar symmetry(Fig. 5a and 5b). However, upon adsorption of acetonitrile, a new cupric ion species due to complex formation with acetonitrile shows ESR parameters rather different form those observed for NH_3, pyridine or aniline adsorption. The ESR parameters are farely consistent with octahedral symmetry. Thus Cu(II) is likely to have an octahedral complex with six aniline molecules.

A new cupric ion species observed upon C_6D_6 corresponds to a complex with one directly interacting benzene molecule via π -bonding based on ESEM data. Upon adsorption of ethylene, ESR shows that only a small amount of Cu(II) forms a new species due to interaction with ethylene. ESEM analysis indicates that Cu(II) interacts only weakly with one molecule of ethylene at a distance greater than for direct coordination.

In general, it is found in the present work that Cu(II) are coordinated to more adsorbate molecules, as expected in a large mesopore. which is not likely to cause restriction for Cu(II) to form favored coordination complexes.

Table 2. ESR parameters at 77 K of tetraammonia complexes of Cu(II), $[Cu(NH_3)_4]^{2+}$, with square planar symmetry in various molecular sieves.

matrix	$g_{||}$[a]	$A_{||}$[b]	ref	
AlMCM-41		2.281	170	this work
pure siliceous MCM-41		2.289	178	20
K-L gallosilicate		2.254	175	22
K-L aluminosolicate		2.255	177	23
ZSM-5 zeolite		2.246	183	19, 24
SAPO-11[c]	2.226	190	25	
X zeolite	2.228	178	26	
Y zeolite	2.235	175	27	
rho zeolite	2.239	175	28	

[a]Estimated uncertainty is ± 0.008. [b]The unit of $A_{||}$ is $1x10^{-4}cm^{-1}$ and the estimated uncertainty is ± $6x10^{-}$ cm^{-1}. [c]SAPO-n represents silicoaluminophosphate molecular sieves.

CONCLUSIONS

The combination of ESR and ESEM spectroscopic measurements has provided fairly good information on probable locations and ligand coordination of Cu(II) ions ion-exchanged into Cu-AlMCM-41. The Cu(II) species in fresh hydrated AlMCM-41 is an octahedrally coordinated hexaaquo species $[Cu(H_2O)_6]^{2+}$ which resides in the mesopore channel with rotational freedom at room temperature. Upon further evacuation treatments, the fully hydrated cupric ion loses some of its coordinated water and becomes anchored to the internal surface of the channel by partial coordination to channel surface oxygens. When completely dehydrated, it is likely that the cupric ions are still located in somewhat exposed sites on the wall of the mesopore. Cu(II) forms a hexagonally coordinated species, $[Cu(CH_3OH)_6]^{2+}$ inside a large mesopore channel. Cu(II) also forms a complex with four molecules of ammonia, pyridine or aniline, but with six molecules of acetonitrile. In general, it is found that Cu(II) are coordinated with maximum number of adsorbate molecules for the formation of favorable complexes in a wide open mesopore. Cu(II) coordinates with one benzene molecule, and interacts only weakly with one ethylene molecule.

Acknowledgment

This research was supported by the Korea Science and Engineering Foundation (97-05-02-06-01-3) and Korean Ministry of Science and Technology(1997). The authors are also grateful to Prof. Larry Kevan at the Department of Chemistry in University of Houston for ESEM measurements.

REFERENCES

1. C. T. Kresge, M. E. Leonowicz, W. J. Roth, J. C. Vartuli and J. S. Back *Nature* **392**, 710 (1992).
2. J.S. Back, J.C. Vartuli, W. J. Roth, M. E. Leonowicz, C. T. Kresge, K. D. Schmitt, C. T-W. Chu, D. H. Olson, E. W. Sheppard, S. B. McCullen, J. B. Higgins and J. L. Schlenker *J. Am. Chem. Soc.* **114**, 10834 (1992).
3. Q. Hou, D. I. Margolese, U. Ciesla, P. Feng, T. E. Gier, P. Sieger, R. Leon, P. M. Petroff, F. Schuth and G. D. Stucky *Nature* **386**, 317 (1994).
4. N. Cousttel, F. D, Renzo and F. Fajula *J. Chem. Soc. Chem. Commun.* 967 (1994).
5. A. Sayari *Chem. Mater.* **8**, 1840 (1996).
6. J. L. Casci, Advanced Zeolite Science and Application Studies: Surface Science and Catalysis Vol. 85, pp329-356, J. C. Jansen, M. Stocker, H. G. Karge, J. Weitkamp, Eds., Elsevier, Amsterdam, 1994.
7. Z. Luan, C. F. Cheng, W. Zhou; J. Klinowski *J. Phys. Chem.* **99**, 1018 (1995).
8. R. Ryoo and J. M. Kim *J. Chem. Soc. Chem. Commun.* 711 (1995).
9. R. Ryoo and S. Jun *J. Phys. Chem. B* **101**, 317 (1997).

10. J. M. Kim, J. H. Kwak, S. Jun and R. Ryoo *J. Phys. Chem.* **99**, 16742 (1995).
11. R. Mokaya and W. Jones *Chem Commun.* 983 (1996).
12. A. Poppl, M. Hartmann and L. Kevan *J. Phys. Chem.* **99**, 17251 (1995).
13. J. S. Yu and L. Kevan *J. Phys. Chem.* **94**, 7612 (1990).
14. L. Kevan, Modern Pulsed and Continuous-Wave Electron Spin Resonance: L. Kevan and M. K. Bowman Eds., Chapter 5, Wiley-Interscience, New York, 1990.
15. H. Tominage, Y. Ono and T. Keii *J. Catal.* **40**, 1075 (1975).
16. B. J. Hathaway and D. E. Billing *Coord. Chem. Rev.* **5**, 143 (1970).
17. (a)J. S. Yu, J. M. Comets and L. Kevan *J. Phys. Chem.* **97**, 11047 (1993).
(b) J S Yu, S. J,. Kim, S. B. Hong and L. Kevan *J. Chem. Soc., Faraday Trans.* **92**, 855 (1996).
18. F. Ucun, F. Koksal and R. Tapramaz *Zeolites* **12**, 420 (1992).
19. C. E. Sass and L. Kevan *J. Phys. Chem.* **92**, 5192 (1988).
20. A. Poppl, M. Newhouse and L. Kevan *J. Phys. Chem.* **99**, 10019 (1995).
21. K.F. Purcell and J. C. Kolts, Inorganic Chemistry, Saunders Company: Philadelphia, Chapter 9, 1977.
22. J. S. Yu, S. B. Hong and L. Kevan *Appl. Magn. Reson.* **10**, 575 (1996).
23. J. S. Yu and L. Kevan *J. Phys. Chem.* **98**, 12436 (1994).
24. Y. Sendoda and Y. Ono *Zeolites* **6**, 209 (1986).
25. C, W. Lee, X. Chen and L. Kevan *J. Phys. Chem.* **95**, 8626 (1991).
26. P. Gallezot, Y. Ben Taarit and B. Imelik *J. Catal.* **26**, 295 (1972).
27. E. F. Vansant and J. H. Lunsford *J. Phys. Chem.* **76**, 2860 (1972).
28. M. W. Anderson and L. Kevan. *J. Phys. Chem.* **91**, 2926 (1987).